Supporting Information for:

An NCN-pincer ligand dysprosium single-ion magnet showing magnetic relaxation *via* the second excited state

Yun-Nan Guo[1, 3], Liviu Ungur[4], Garrett E. Granroth[5], Annie K. Powell[6], Chunji Wu[2], Stephen E. Nagler[5], Jinkui Tang[1,]*, Liviu F. Chibotaru[4,]* & Dongmei Cui[2,]*

[1] State Key Laboratory of Rare Earth Resource Utilization, Changchun Institute of Applied Chemistry, Chinese Academy of Sciences, Changchun 130022, P. R. China. Fax: (+)86–431–85262878; E-mail: tang@ciac.ac.cn; [2] State Key Laboratory of Polymer Physics and Chemistry, Changchun Institute of Applied Chemistry, Chinese Academy of Sciences, Changchun 130022, P. R. China; [3] School of Science, Xi'an Jiaotong University, Xi'an 710049, P. R. China; [4] Division of Quantum and Physical Chemistry, Department of Chemistry, Katholieke Universiteit Leuven, Celestijnenlaan 200F, 3001 Leuven, Belgium; [5] Oak Ridge National Laboratory, Oak Ridge, Tennessee 37831, USA; [6] Institute of Inorganic Chemistry, Karlsruhe Institute of Technology, Engesserstrasse 15, 76131 Karlsruhe, Germany and Institute of Nanotechnology, Karlsruhe Institute of Technology, Hermann-von-Helmholtz-Platz 1, Eggensteinn-Leopoldshafen, 76344 Karlsruhe, Germany

Contents

1 Computational details

The ab initio calculations of DyNCN have been done with Molcas 7.8 package.[1] In these calculations, the relativistic effects are taken into account in two steps, both based on the Douglas-Kroll Hamiltonian.[2] In the first step, scalar relativistic effects are already taken into account in the basis set generation. Further, spin-free eigenstates are obtained in the Complete Active Space Self Consistent Field (CASSCF) method.[3] The active space of the CASSCF included the 9 electrons spanning seven 4f orbitals of the Dy^{3+} ion, unless otherwise specified. The spin-orbit coupling is considered in the next step (RASSI),[4] which uses spin-free eigenstates as input, and in their basis computes the matrix elements of the magnetic moment. In the last step, the SINGLE_ANISO module computes all magnetic properties and parameters of the pseudo-spin Hamiltonians on the basis of the above calculated spin-orbit eigenstates and matrix elements of the magnetic moment. This method has been successfully applied for the elucidation of the local electronic and magnetic properties of other lanthanide complexes.[5]

Two structural models for the mononuclear Dy fragments have been employed: fragment **A** (small), **B** (larger) and **C** (entire molecule). Structure of the structural model **A** and **B** are shown in Figures S1 and S2 respectively.

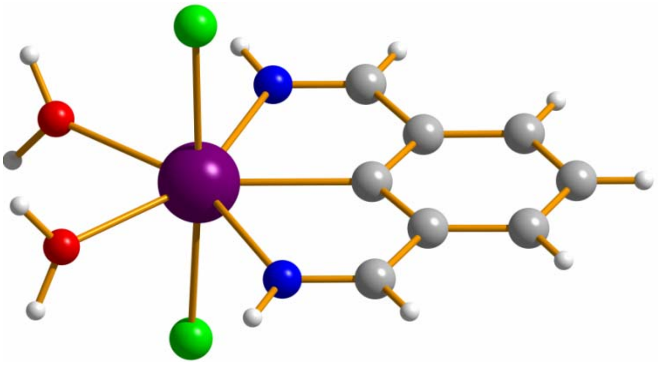

Fig. S1 Structure of the fragment **A** of the molecule.

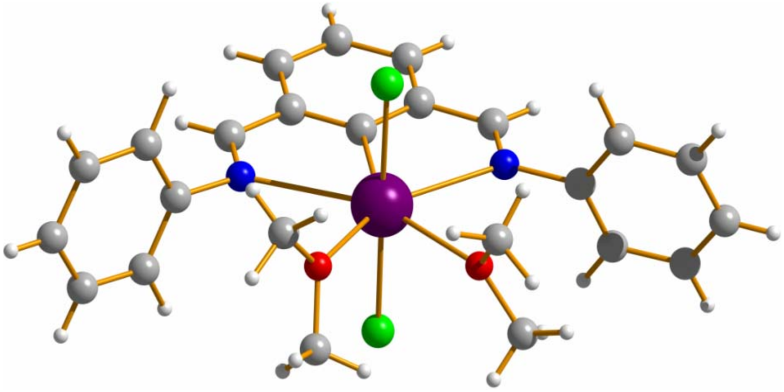

Fig. S2 Structure of the fragment **B** of the molecule.

Three basis set approximations have been employed: **1** – small, **2** – larger, and **3** – even larger. Table S1 shows the contractions of the employed basis sets for all elements.
All in all we have the following computational models: **A1**, **A2**, **B1**, **B2**, **C1**, **C2** and **C3**;

Table S1. Contractions of the employed basis sets in computational approximations **1** and **2**.

Basis 1	Basis 2	Basis 3
Dy.ANO-RCC...7s6p4d3f1g.	Dy.ANO-RCC...8s7p5d4f2g1h.	Dy.ANO-RCC...9s8p5d4f3g2h.
Cl.ANO-RCC...4s3p.	Cl.ANO-RCC...5s4p2d.	Cl.ANO-RCC...6s5p3d2f1g.
O.ANO-RCC...3s2p.	O.ANO-RCC...4s3p2d.	O.ANO-RCC...5s4p3d2f1g.
N.ANO-RCC...3s2p.	N.ANO-RCC...4s3p2d.	N.ANO-RCC...5s4p3d2f1g.
C.ANO-RCC...3s2p. (all)	C.ANO-RCC...4s3p2d. (closest)	C.ANO-RCC...5s4p3d2f1g. (closest)
H.ANO-RCC...2s.	C.ANO-RCC...3s2p. (distant)	C.ANO-RCC...4s3p2d. (medium)
	H.ANO-RCC...2s.	C.ANO-RCC...3s2p. (distant)
		H.ANO-RCC...2s.

Active space of the CASSCF method included 9 electrons in 7 orbitals (4*f* orbitals of Dy^{3+} ion).
We have mixed 21 sextets, 128 quartet and 130 doublet states by spin-orbit coupling.
On the basis of the resulting spin-orbital multiplets SINGLE_ANISO program computed local magnetic properties (g-tensors, magnetic axes, local magnetic susceptibility, etc.)

Table S2. Cartesian atomic coordinates of the structural model **A** (in Angstrom).

Atom	X	Y	Z
Dy1	0.00000000	0.00000000	0.07483997
Cl2	0.12799602	-2.59167289	0.15403593
Cl3	-0.12799602	2.59167289	0.15403593
O4	-1.49433608	0.03051414	2.01415102
O5	1.49433608	-0.03051414	2.01415102
N6	-2.43535991	-0.07028578	-1.01467016
N7	2.43535991	0.07028578	-1.01467016
C8	-2.43096661	-0.06761297	-2.29813968
C9	-1.18700315	-0.04373029	-3.06181500
C10	0.00000000	0.00000000	-2.31843365
C11	-1.19090729	-0.03923611	-4.45622958
C12	0.00000000	0.00000000	-5.14869925
C13	2.43096661	0.06761297	-2.29813968
C14	1.18700315	0.04373029	-3.06181500
C15	1.19090729	0.03923611	-4.45622958
H16	-3.24172096	-0.08087504	-2.75457711
H17	-1.99819548	-0.06151598	-4.91853599
H18	0.00000000	0.00000000	-6.07826182
H19	3.24172096	0.08087504	-2.75457711
H20	1.99819548	0.06151598	-4.91853599
H21	-3.33567767	-0.05887911	-0.57958646
H22	3.33567767	0.05887911	-0.57958646
H23	-2.02895769	0.74083792	2.37639384
H24	-1.55819788	-0.72295302	2.60559748
H25	1.55819788	0.72295302	2.60559748
H26	2.02895769	-0.74083792	2.37639384

Table S3. Cartesian atomic coordinates of the structural model B (in Angstrom).

Atom	X	Y	Z
Dy1	0.00000000	0.00000000	0.07483997
Cl2	0.12799602	-2.59167289	0.15403593
Cl3	-0.12799602	2.59167289	0.15403593
O4	-1.49433608	0.03051414	2.01415102
O5	1.49433608	-0.03051414	2.01415102
N6	-2.43535991	-0.07028578	-1.01467016
N7	2.43535991	0.07028578	-1.01467016
C8	-4.29501058	-1.26128941	0.05461671
C9	-2.43096661	-0.06761297	-2.29813968
C10	-6.21907737	-0.03392313	0.84473783
C11	-5.53739361	-1.22038381	0.67192093
C12	-4.41005248	1.16587624	-0.22263986
C13	-3.73937669	-0.05376440	-0.38449660
C14	-5.65114197	1.14066303	0.40371533
C15	-2.30447839	1.10690786	2.56307802
C16	-1.59141548	-1.11486761	2.91323730
C17	-1.18700315	-0.04373029	-3.06181500
C18	0.00000000	0.00000000	-2.31843365
C19	-1.19090729	-0.03923611	-4.45622958
C20	0.00000000	0.00000000	-5.14869925

C21	4.29501058	1.26128941	0.05461671
C22	2.43096661	0.06761297	-2.29813968
C23	6.21907737	0.03392313	0.84473783
C24	5.53739361	1.22038381	0.67192093
C25	4.41005248	-1.16587624	-0.22263986
C26	3.73937669	0.05376440	-0.38449660
C27	5.65114197	-1.14066303	0.40371533
C28	1.18700315	0.04373029	-3.06181500
C29	1.19090729	0.03923611	-4.45622958
C30	2.30447839	-1.10690786	2.56307802
C31	1.59141548	1.11486761	2.91323730
H32	-3.24172096	-0.08087504	-2.75457711
H33	-7.05278172	-0.02622923	1.25584971
H34	-5.91992792	-2.01241461	0.97548187
H35	-6.11177422	1.93855830	0.52823683
H36	-2.80552726	1.55172598	1.86311302
H37	-1.74658841	1.76128373	3.01223225
H38	-0.70838188	-1.42719360	3.16291670
H39	-2.06912507	-1.84308213	2.48671049
H40	-1.99819548	-0.06151598	-4.91853599
H41	0.00000000	0.00000000	-6.07826182
H42	3.24172096	0.08087504	-2.75457711
H43	7.05278172	0.02622923	1.25584971
H44	5.91992792	2.01241461	0.97548187
H45	6.11177422	-1.93855830	0.52823683
H46	1.99819548	0.06151598	-4.91853599
H47	2.80552726	-1.55172598	1.86311302
H48	1.74658841	-1.76128373	3.01223225
H49	0.70838188	1.42719360	3.16291670
H50	2.06912507	1.84308213	2.48671049
H51	-4.00433890	2.09463687	-0.56571446
H52	-3.81137740	-2.20305406	-0.10055514
H53	3.81137740	2.20305406	-0.10055514
H54	4.00433890	-2.09463687	-0.56571446
H55	-2.96480471	0.63144184	3.25791701
H56	-2.12481130	-0.76804949	3.77353149
H57	2.96480471	-0.63144184	3.25791701
H58	2.12481130	0.76804949	3.77353149

Table S4. Cartesian atomic coordinates of the structural model C -- the entire molecule (in Angstrom).

Atom	X	Y	Z
Dy1	0.00000000	0.00000000	0.07483997
Cl2	0.12799602	-2.59167289	0.15403593
Cl3	-0.12799602	2.59167289	0.15403593
O4	-1.49433608	0.03051414	2.01415102
O5	1.49433608	-0.03051414	2.01415102
N6	-2.43535991	-0.07028578	-1.01467016
N7	2.43535991	0.07028578	-1.01467016
C8	-4.29501058	-1.26128941	0.05461671
C9	-2.43096661	-0.06761297	-2.29813968
C10	-3.61511330	-2.58523337	-0.16352573
C11	-6.21907737	-0.03392313	0.84473783
C12	-5.53739361	-1.22038381	0.67192093
C13	-4.03151334	-3.25398846	-1.44190408
C14	-4.41005248	1.16587624	-0.22263986
C15	-3.73937669	-0.05376440	-0.38449660
C16	-3.83841851	2.47446230	-0.70601805
C17	-5.65114197	1.14066303	0.40371533
C18	-4.36563696	2.88418842	-2.08303780
C19	-2.30447839	1.10690786	2.56307802
C20	-1.59141548	-1.11486761	2.91323730
C21	-3.23295974	0.43835760	3.54008746
C22	-2.34045132	-0.62783867	4.12132923
C23	-1.18700315	-0.04373029	-3.06181500
C24	0.00000000	0.00000000	-2.31843365
C25	-1.19090729	-0.03923611	-4.45622958
C26	0.00000000	0.00000000	-5.14869925
C27	4.29501058	1.26128941	0.05461671
C28	2.43096661	0.06761297	-2.29813968
C29	3.61511330	2.58523337	-0.16352573
C30	6.21907737	0.03392313	0.84473783
C31	5.53739361	1.22038381	0.67192093
C32	4.03151334	3.25398846	-1.44190408
C33	4.41005248	-1.16587624	-0.22263986
C34	3.73937669	0.05376440	-0.38449660

C35	3.83841851	-2.47446230	-0.70601805
C36	5.65114197	-1.14066303	0.40371533
C37	4.36563696	-2.88418842	-2.08303780
C38	1.18700315	0.04373029	-3.06181500
C39	1.19090729	0.03923611	-4.45622958
C40	2.30447839	-1.10690786	2.56307802
C41	1.59141548	1.11486761	2.91323730
C42	3.23295974	-0.43835760	3.54008746
C43	2.34045132	0.62783867	4.12132923
H44	-3.24172096	-0.08087504	-2.75457711
H45	-2.65422315	-2.44952586	-0.17710218
H46	-3.82050548	-3.17262876	0.58084558
H47	-7.05278172	-0.02622923	1.25584971
H48	-5.91992792	-2.01241461	0.97548187
H49	-4.98589461	-3.36617408	-1.44890444
H50	-3.60908190	-4.11359499	-1.50618009
H51	-3.76829847	-2.71071054	-2.18818458
H52	-2.87097285	2.40061294	-0.74710096
H53	-4.05558435	3.17101052	-0.06615713
H54	-6.11177422	1.93855830	0.52823683
H55	-4.11660906	2.21941777	-2.73004050
H56	-3.98683576	3.73004115	-2.33179796
H57	-5.32273982	2.95685398	-2.05036947
H58	-2.80552726	1.55172598	1.86311302
H59	-1.74658841	1.76128373	3.01223225
H60	-0.70838188	-1.42719360	3.16291670
H61	-2.06912507	-1.84308213	2.48671049
H62	-4.00246367	0.05370134	3.09284242
H63	-3.53698953	1.05831578	4.22209195
H64	-1.73742108	-0.26012373	4.78622174
H65	-2.86064261	-1.34055641	4.52459223
H66	-1.99819548	-0.06151598	-4.91853599
H67	0.00000000	0.00000000	-6.07826182
H68	3.24172096	0.08087504	-2.75457711
H69	2.65422315	2.44952586	-0.17710218
H70	3.82050548	3.17262876	0.58084558
H71	7.05278172	0.02622923	1.25584971
H72	5.91992792	2.01241461	0.97548187
H73	4.98589461	3.36617408	-1.44890444
H74	3.60908190	4.11359499	-1.50618009
H75	3.76829847	2.71071054	-2.18818458
H76	2.87097285	-2.40061294	-0.74710096
H77	4.05558435	-3.17101052	-0.06615713
H78	6.11177422	-1.93855830	0.52823683
H79	4.11660906	-2.21941777	-2.73004050
H80	3.98683576	-3.73004115	-2.33179796
H81	5.32273982	-2.95685398	-2.05036947
H82	1.99819548	0.06151598	-4.91853599
H83	2.80552726	-1.55172598	1.86311302
H84	1.74658841	-1.76128373	3.01223225
H85	0.70838188	1.42719360	3.16291670
H86	2.06912507	1.84308213	2.48671049
H87	4.00246367	-0.05370134	3.09284242
H88	3.53698953	-1.05831578	4.22209195
H89	1.73742108	0.26012373	4.78622174
H90	2.86064261	1.34055641	4.52459223

2 Electronic and magnetic properties of individual Dy centers

Table S5. Energies of the lowest Kramers doublets (cm^{-1}). (roots corresponding to the ^{6}H, ^{6}F and ^{6}P ionic multiplets were optimized *together* in a single state-average CASSCF calculation; *method 1*)

A1	A2	B1	B2	C1	C2	C3
0.000	0.000	0.000	0.000	0.000	0.000	0.000
143.600	44.004	169.284	152.165	173.422	157.205	160.251
283.435	126.845	342.071	178.238	350.935	221.422	216.679
326.412	226.299	444.122	298.166	457.187	312.608	316.002
359.021	279.699	464.155	371.700	497.952	397.193	399.101
433.162	356.902	528.949	445.090	548.205	462.642	467.423
468.077	400.951	585.554	505.520	609.094	518.103	525.846
512.690	436.098	628.383	539.766	657.864	561.729	571.403
3611.383	3589.726	3626.119	3605.682	3629.033	3609.451	3611.387
3757.832	3668.796	3802.422	3752.328	3809.952	3766.014	3767.415
3828.252	3709.364	3893.524	3790.244	3904.834	3818.538	3818.717
3874.298	3749.716	3960.161	3830.131	3976.530	3852.617	3854.376
3908.999	3800.465	4013.893	3884.744	4035.535	3905.056	3908.683
3940.513	3858.332	4055.591	3953.250	4079.347	3972.171	3977.805
3978.237	3928.255	4098.081	4028.663	4128.000	4043.388	4051.570
…	…	…	…	…	…	…

Table S6. Energies of the lowest Kramers doublets (cm^{-1}). (roots corresponding to the ^{6}H, ^{6}F and ^{6}P ionic multiplets were optimized *separately* in three different CASSCF calculations; *method 2*)

A1	A2	B1	B2	C1	C2	C3
0.000	0.000	0.000	0.000	0.000	0.000	0.000
154.921	59.269	184.185	166.097	189.082	172.300	176.025
308.508	135.599	373.517	216.210	383.749	266.583	262.595
372.970	243.103	491.334	326.555	505.677	344.067	348.429
395.360	304.860	527.667	412.586	564.645	442.294	445.506
471.266	394.807	581.309	498.503	604.761	520.285	526.797
512.274	452.830	644.284	573.093	670.414	587.106	597.470
560.421	486.339	692.225	607.687	725.904	632.845	645.697
3619.224	3595.507	3636.334	3614.472	3639.735	3619.049	3621.242
3779.335	3686.362	3829.859	3777.500	3838.472	3793.124	3795.172
3857.800	3727.391	3931.675	3825.958	3944.640	3857.739	3859.063
3910.739	3774.599	4007.712	3869.822	4026.215	3897.483	3900.148
3952.137	3833.413	4070.142	3933.188	4094.127	3957.825	3962.878
3986.623	3901.896	4117.637	4012.819	4144.687	4035.239	4042.998
4028.978	3984.506	4165.514	4101.186	4199.749	4118.458	4129.523
…	**…**	**…**	**…**	**…**	**…**	**…**

Table S7. Energies (cm^{-1}) and *g* tensors of the lowest Kramers doublets (KD) (*method 1*).

KD		**A1**		**A2**		**B1**		**B2**		**C1**		**C2**		**C3**	
		E	***g***	**E**	***g***	**E**	***g***	**E**	***g***	**E**	***g***	**E**	***g***	**E**	***g***
1	g_X	0.000	0.0110	0.000	0.0027	0.000	0.0066	0.000	0.0011	0.000	0.0069	0.000	0.0016	0.000	0.0016
	g_Y		0.0186		0.0232		0.0108		0.0032		0.0111		0.0034		0.0035
	g_Z		19.7006		19.7908		19.7124		19.8005		19.7051		19.7893		19.7869

2	g_X	143.600	0.1866	44.004	0.0008	169.284	0.1128	152.165	0.1179	173.422	0.1162	157.205	0.0026	160.251	0.0064
	g_Y		0.2550		0.0130		0.1460		0.4091		0.1515		0.0332		0.0583
	g_Z		16.7450		19.8253		16.8063		16.8443		16.7852		17.0289		17.0102
3	g_X	283.435	2.4192	126.845	0.2858	342.071	1.4375	178.238	0.0854	350.935	1.4687	221.422	0.2157	216.679	0.1711
	g_Y		3.8642		0.3192		2.0825		0.3255		2.1617		0.2773		0.2670
	g_Z		12.1846		16.9593		13.2580		19.2958		13.1859		19.5973		19.5914
4	g_X	326.412	0.1955	226.299	9.2981	444.122	5.7547	298.166	2.7778	457.187	5.7535	312.608	1.9635	316.002	2.1349
	g_Y		0.4470		8.2202		6.5631		3.2095		6.0982		2.2290		2.3052
	g_Z		19.2568		4.3589		7.4275		12.7155		7.9628		13.1812		13.1412
5	g_X	359.021	9.1850	279.699	1.8922	464.155	0.1106	371.700	8.3936	497.952	0.1618	397.193	8.3293	399.101	8.4013
	g_Y		6.2810		2.6270		0.4679		7.5527		0.4531		7.2071		7.3276
	g_Z		3.0625		9.5480		18.3404		3.9321		18.8972		5.3714		5.1198
6	g_X	433.162	0.7499	356.902	2.2510	528.949	0.9971	445.090	0.7931	548.205	0.9250	462.642	0.3015	467.423	0.0586
	g_Y		2.6993		2.7421		1.8170		1.6862		1.6852		0.7924		0.9964
	g_Z		11.4785		14.0593		11.6430		14.1355		11.8754		14.4359		14.3222
7	g_X	468.077	1.1582	400.951	0.0212	585.554	1.1789	505.520	0.3853	609.094	1.1339	518.103	0.3900	525.846	0.4573
	g_Y		2.0754		0.2793		1.3381		0.7648		1.2925		0.8495		0.7984
	g_Z		17.3457		19.3168		17.4645		19.3723		16.9870		19.2337		19.3234
8	g_X	512.690	0.2736	436.098	0.2124	628.383	0.0853	539.766	0.2601	657.864	0.0083	561.729	0.2303	571.403	0.1844
	g_Y		0.5845		0.3880		0.1606		0.5962		0.1064		0.6035		0.4624
	g_Z		18.3891		18.4214		18.8871		18.8265		18.9738		18.9091		19.0735

Table S8. Energies (cm^{-1}) and *g* tensors of the lowest Kramers doublets (KD) (*method 2*).

KD		**A1**		**A2**		**B1**		**B2**		**C1**		**C2**		**C3**	
		E	***g***	**E**	***g***	**E**	***g***	**E**	***g***	**E**	***g***	**E**	***g***	**E**	***g***
1	g_X	0.000	0.0085	0.000	0.0035	0.000	0.0050	0.000	0.0008	0.000	0.0052	0.000	0.0010	0.000	0.0010
	g_Y		0.0140		0.0146		0.0079		0.0021		0.0082		0.0021		0.0021
	g_Z		19.7207		19.8209		19.7321		19.8216		19.7255		19.8113		19.8101
2	g_X	154.921	0.1469	59.269	0.0285	184.185	0.0883	166.097	0.0705	189.082	0.0916	172.300	0.0030	176.025	0.0087
	g_Y		0.1957		0.0345		0.1124		0.1697		0.1175		0.0220		0.0346
	g_Z		16.8010		19.8135		16.8452		17.0243		16.8239		17.0680		17.0586
3	g_X	308.508	1.9425	135.599	0.3428	373.517	1.1524	216.210	0.1971	383.749	1.1898	266.583	0.4716	262.595	0.4261
	g_Y		2.9584		0.4139		1.5976		0.3917		1.6770		0.5064		0.4374
	g_Z		12.7828		16.9041		13.5191		19.4391		13.4469		19.4033		19.4439
4	g_X	372.970	0.6275	243.103	8.7862	491.334	7.3010	326.555	2.9079	505.677	5.6090	344.067	1.7498	348.429	1.9619
	g_Y		1.0567		8.5153		6.7837		3.0258		6.6107		2.4932		2.5423
	g_Z		18.7071		4.5239		5.6723		12.5908		7.6501		12.8537		12.8581
5	g_X	395.360	3.6619	304.860	1.1972	527.667	0.3801	412.586	8.4348	564.645	0.3286	442.294	8.0066	445.506	8.0980
	g_Y		5.8769		2.5716		0.9307		7.2532		0.9465		7.1333		7.2355
	g_Z		9.8221		9.8550		18.6080		4.3054		17.9682		5.6743		5.4345
6	g_X	471.266	1.2680	394.807	1.9168	581.309	0.3400	498.503	0.4067	604.761	0.3369	520.285	0.4246	526.797	0.4681
	g_Y		2.1834		2.4444		2.3310		1.2896		1.9522		0.7080		0.6001
	g_Z		11.4567		13.8583		11.9459		13.9630		12.8677		14.1059		14.0454
7	g_X	512.274	1.2264	452.830	0.1886	644.284	1.1129	573.093	0.5387	670.414	1.0393	587.106	0.5236	597.470	0.5562
	g_Y		1.9901		0.3076		1.1364		0.6054		1.1414		0.6956		0.6565
	g_Z		17.3740		19.6369		17.3164		19.4832		16.7753		19.4339		19.4099

8	g_X g_Y g_Z	560.421	0.1596 0.4503 18.6717	486.339	0.1597 0.2736 18.8922	692.225	0.0225 0.1576 18.9929	607.687	0.0859 0.2948 19.2913	725.904	0.1100 0.1505 19.0174	632.845	0.0871 0.3386 19.2604	645.697	0.0587 0.2346 19.3829

Method 2 (the multiplet-specific root optimization at the CASSCF level) is more accurate for the low-lying levels than ***Method 1*** (single-state average CASSCF calculation including all roots from different ionic multiplets) because the orbitals are better optimized when only roots of similar energy are taken into account. A state-average CASSCF calculation including roots which have very different energies is less accurate because for all the roots one single set of orbitals is optimized. This is reflected in the later stage (RASSI) when spin-orbit coupling is included. The best results correspond to C2 and C3 in Tables S6 and S8 and almost do not differ from each other.

Table S9. Angles between the main magnetic axes of the lowest Kramers doublet obtained in different computational approximations (degrees)

	A1	**A2**	**B1**	**B2**	**C1**	**C2**	**C3**
A1	5.467E-06	7.826E-05	4.398E-05	6.864E-05	3.740E-05	7.897E-05	4.017E-05
A2	7.826E-05	8.538E-07	5.925E-05	7.232E-05	7.743E-05	7.862E-05	6.713E-05
B1	4.398E-05	5.925E-05	8.365E-06	2.789E-05	2.160E-05	3.800E-05	1.213E-05
B2	6.864E-05	7.232E-05	2.789E-05	7.143E-06	3.589E-05	1.228E-05	2.996E-05
C1	3.740E-05	7.743E-05	2.160E-05	3.589E-05	9.993E-06	4.515E-05	1.451E-05
C2	7.897E-05	7.862E-05	3.800E-05	1.228E-05	4.515E-05	5.051E-06	3.997E-05
C3	4.017E-05	6.713E-05	1.213E-05	2.996E-05	1.451E-05	3.997E-05	8.873E-06

Table S10. Angle between the main magnetic axes of the lowest Kramers doublet and the Dy-C bond (degrees).

	A1	**A2**	**B1**	**B2**	**C1**	**C2**	**C3**
angle	5.313E-05	6.064E-05	1.145E-05	1.811E-05	2.563E-05	2.807E-05	1.620E-05

Table S11. Angle between the main magnetic axes of the lowest and first excited Kramers doublets (degrees).

	A1	**A2**	**B1**	**B2**	**C1**	**C2**	**C3**
angle	1.943E-04	90.000[a]	2.197E-05	2.756E-05	3.445E-05	3.371E-05	4.106E-05

[a]. Only the A2 model predicts a non-collinear arrangement of the main magnetic axes in the ground and first excited doublets. We can see from the above tables that the approximation A2 gives predictions which differ strongly from all other approximations and, therefore, cannot be trusted. The approximations corresponding to highest accuracy, C2 and C3, give very close results.

Table S12. Comparison of the results predicted by various active spaces of the CASSCF method. All calculations were similar to the A1 model shown above. The calculations involved a state-average orbital optimization for all spin sextet (^{6}H, ^{6}F and ^{6}P). CAS(*n*,*m*) represents an active space of *n* electrons spanning *m* orbitals.

KD		**CAS(9,7)**		**CAS(11,9)**		**CAS(15,11)**		**CAS(15,13)**	
		E	***g***	**E**	***g***	**E**	***g***		
1	g_X	0.000	0.0111	0.000	0.0087	0.000	0.0094	0.000	0.0082
	g_Y		0.0188		0.0143		0.0156		0.0135
	g_Z		19.8036		19.8264		19.8201		19.8312
2	g_X	142.599	0.1847	150.070	0.1506	147.322	0.1606	152.542	0.1489
	g_Y		0.2490		0.2002		0.2141		0.1994
	g_Z		16.8322		16.8842		16.8719		16.8829
3	g_X	285.332	2.4029	298.706	2.0655	294.003	2.1908	301.220	2.0194
	g_Y		3.8316		3.0492		3.3047		3.0310
	g_Z		12.2785		12.7827		12.6226		12.7977
4	g_X	329.343	0.1939	346.647	0.3288	339.412	0.2816	354.868	0.4075
	g_Y		0.4423		0.6738		0.6086		0.7572
	g_Z		19.3622		19.2335		19.2609		19.1610
5	g_X	362.812	9.3287	382.117	3.7903	375.057	3.4892	384.930	3.8011
	g_Y		6.3287		6.0877		6.1777		6.0501
	g_Z		3.0364		9.6003		9.5774		9.6324
6	g_X	439.033	0.8618	454.931	1.0840	448.789	0.9821	458.444	1.1217
	g_Y		2.8775		2.3389		2.5997		2.2374
	g_Z		11.3640		11.7858		11.6301		11.7311
7	g_X	474.408	1.2140	493.241	1.1518	485.836	1.1857	497.919	1.1658
	g_Y		2.2602		2.0520		2.1673		1.9806
	g_Z		17.2676		17.5670		17.4427		17.5957
8	g_X	520.129	0.3163	538.879	0.2554	531.628	0.2875	543.755	0.2095
	g_Y		0.6447		0.6554		0.6648		0.5708
	g_Z		18.4036		18.5269		18.4793		18.6249

We notice minor changes in the local spectrum and anisotropy of individual Kramers doublets upon increasing the size of the active space.

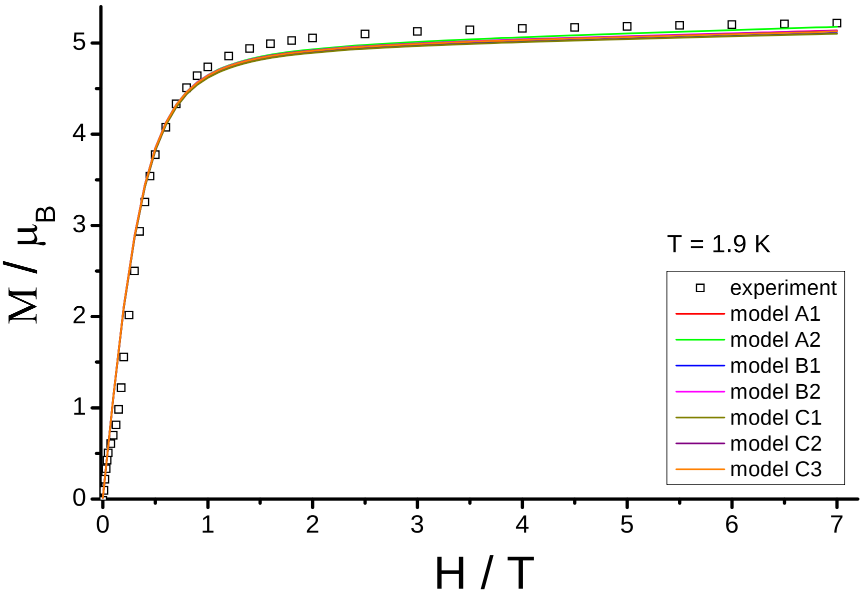

Fig. S3 Measured and calculated molar magnetization at 1.9 K.

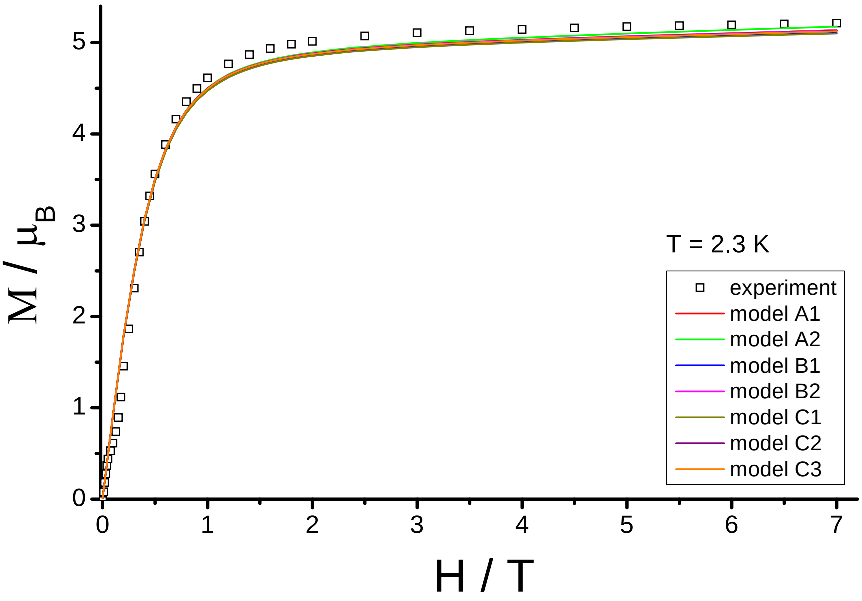

Fig. S4 Measured and calculated molar magnetization at 2.3 K.

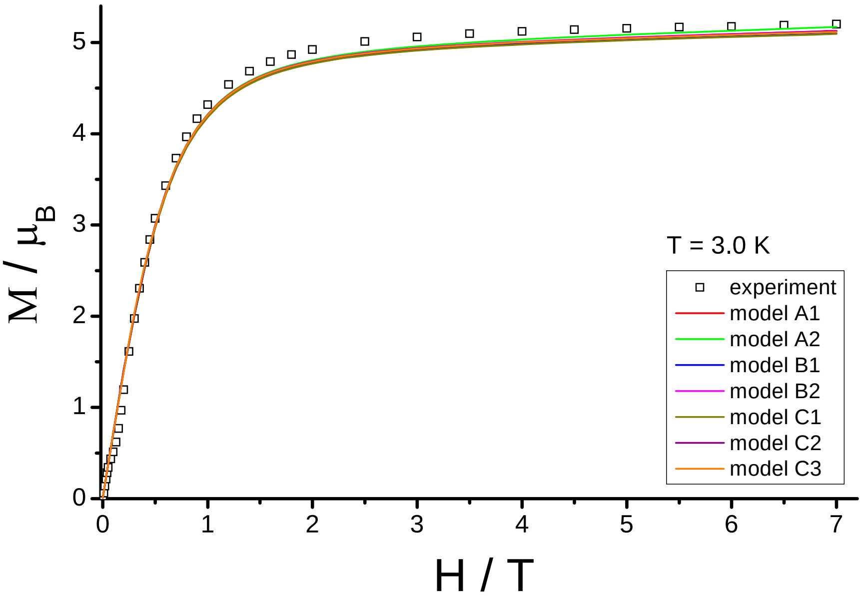

Fig. S5 Measured and calculated molar magnetization at 3.0 K.

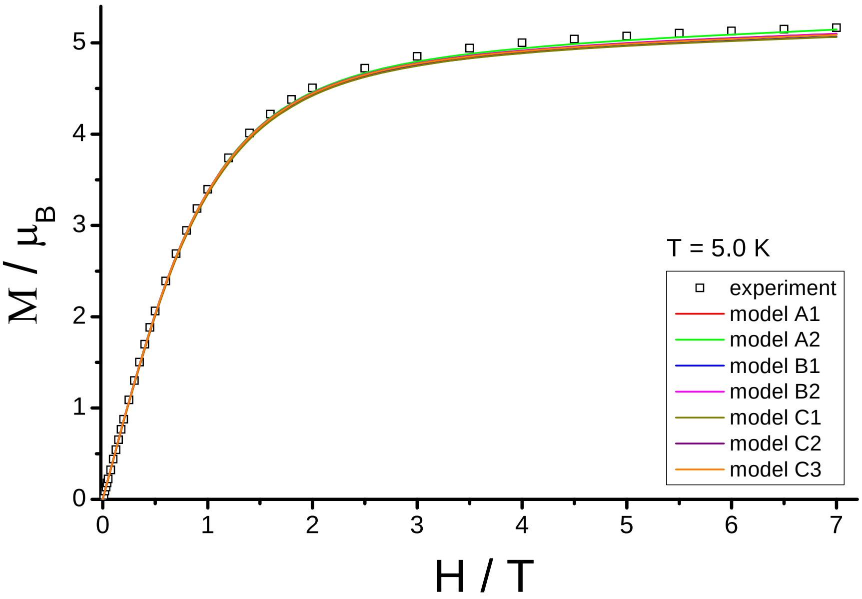

Fig. S6 Measured and calculated molar magnetization at 5.0 K.

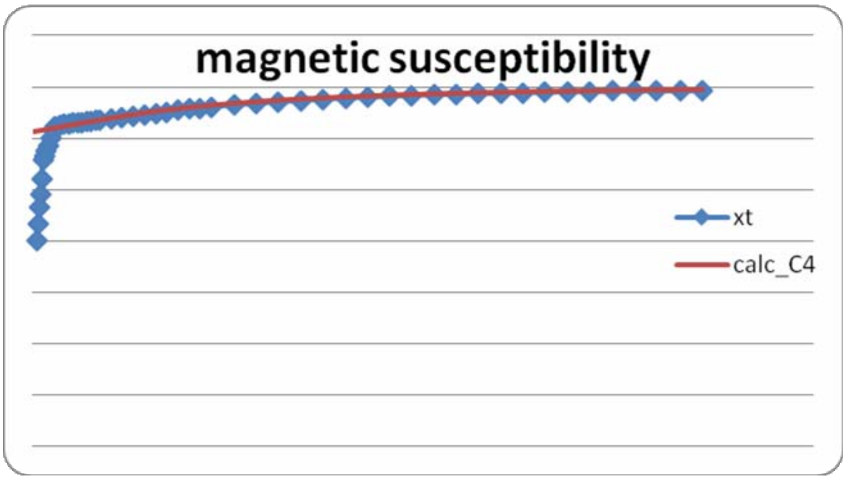

Fig. S7 Ab initio calculations of temperature dependence of powder susceptibility for an individual DyNCN complex (lines) and their comparison with experiment (diamonds). The intermolecular magnetic interaction was not taken into account. The $\chi_{\mathrm{M}}T$ at around 10 K shows a kink, which is not expected for molecular susceptibility. The kink cannot be due to magnetic ordering since intermolecular dipolar interaction is much weaker. This phenomenon may probably a kind of structural phase transition (for instance ordering of solvent molecules) which suddenly changes the crystal field at the Dy site and its magnetic properties. However these changes are not large, otherwise the calculations based on the room temperature geometry would not have sense.

3 Inelastic neutron scattering measurements

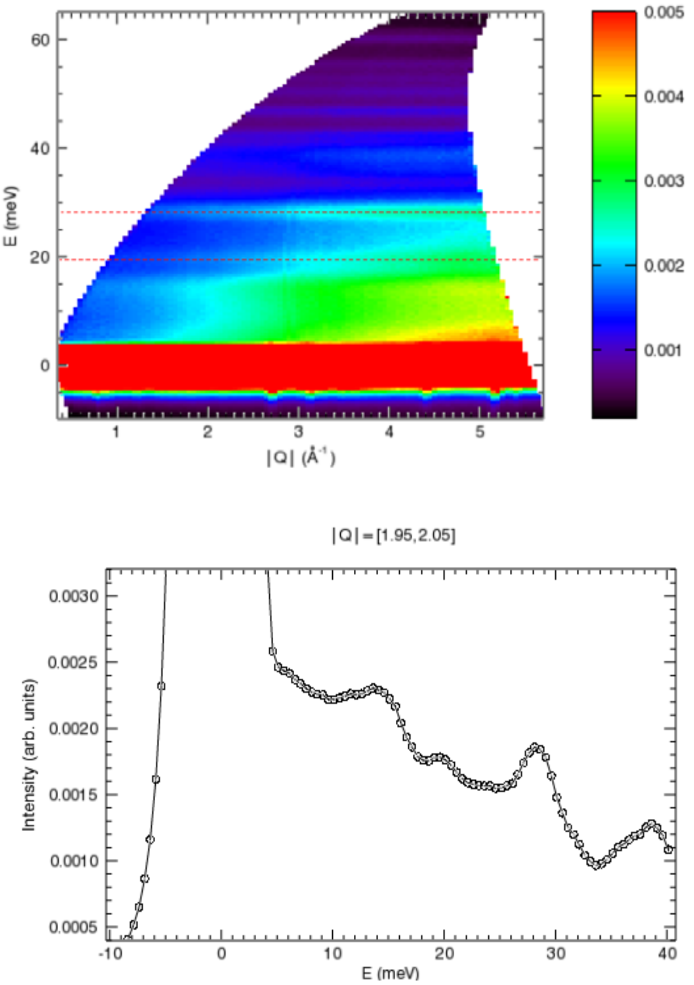

Fig. S8 (Top) Color map of Inelastic neutron scattering spectra of DyNCN taken at the Ei ~ 70 meV Fermi Chopper 1 at 240 Hz. (Bottom) Low Q data of inelastic neutron scattering spectra of **DyNCN** taken at the Ei ~ 70 meV Fermi Chopper 1 at 240 Hz. There are more peaks that are probably libration or rotation motions of the H.

4 Alternating current (ac) magnetic susceptibility measurements

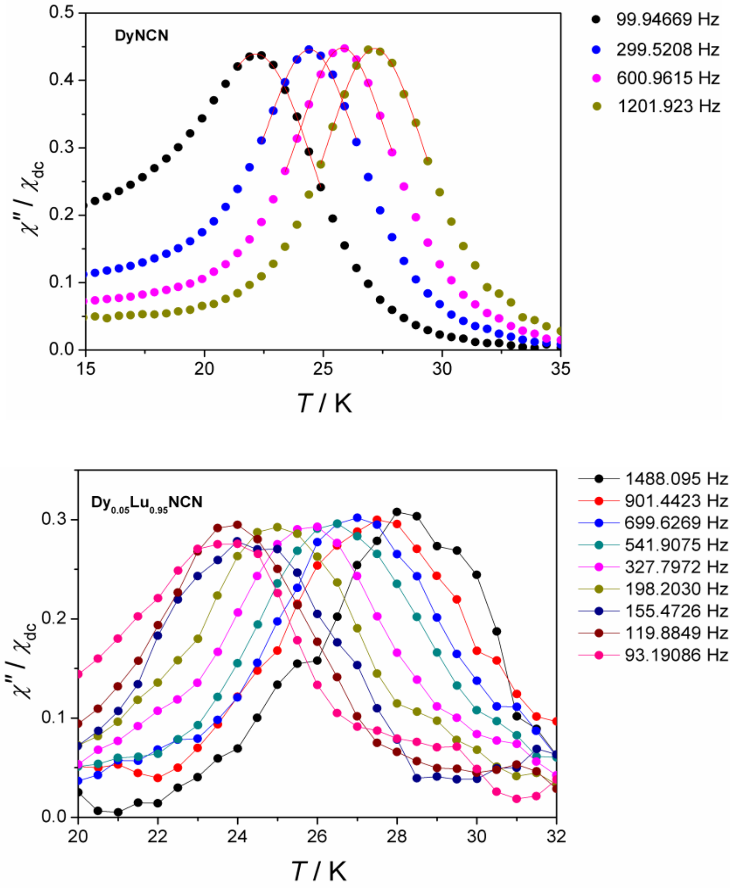

Fig. S9 Temperature dependence of out-of-phase (χ'') component of ac magnetic susceptibility for DyNCN (Top) and $Dy_{0.05}Lu_{0.95}NCN$ (bottom) in zero static field. The χ'' data are normalized at each temperature by the corresponding value of χ_{dc} from the data in Fig. S7.

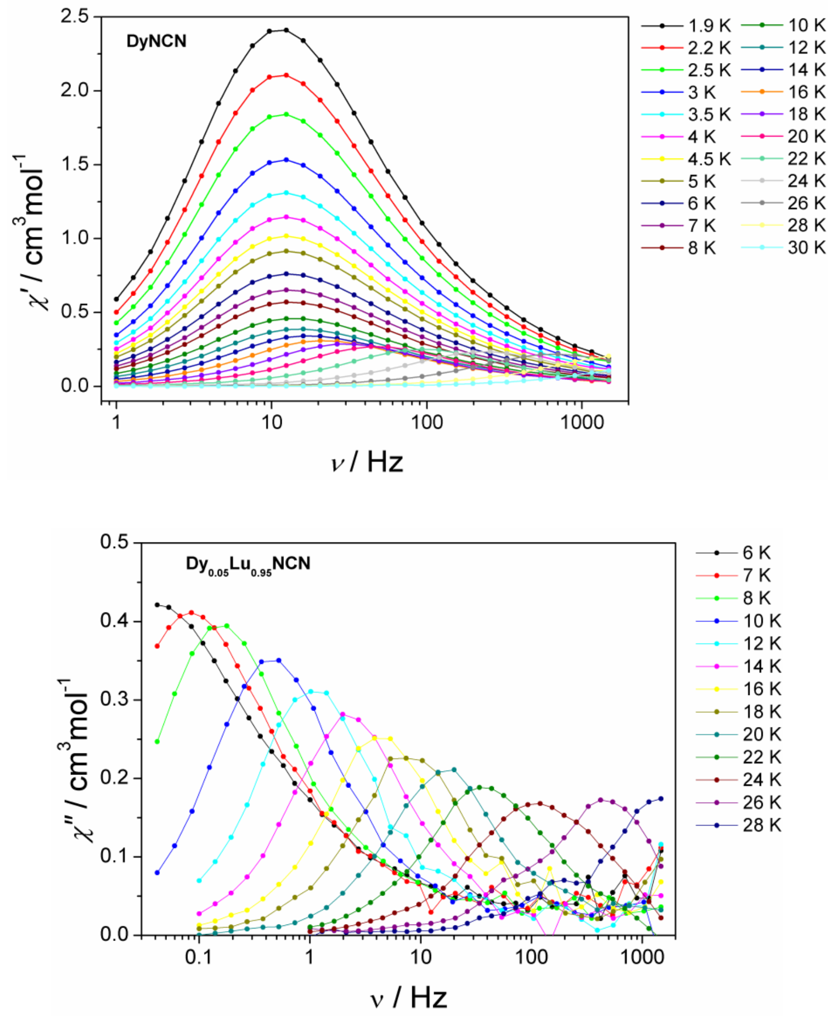

Fig. S10 Frequency dependence of χ'' component of ac magnetic susceptibility for for DyNCN (left) and $Dy_{0.05}Lu_{0.95}NCN$ (right) in zero static field.

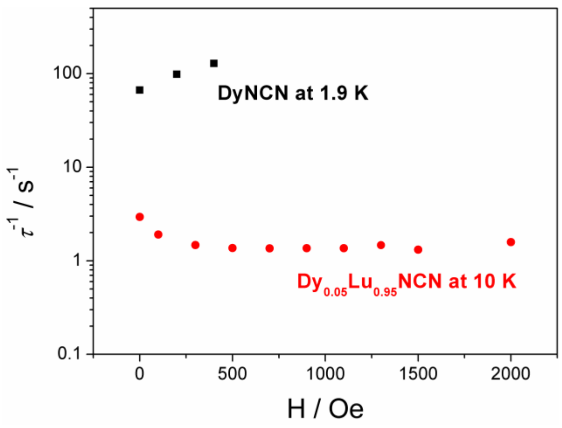

Fig. S11 The dependence of relaxation rate τ^{-1} on the external magnetic field H for DyNCN and $Dy_{0.05}Lu_{0.95}NCN$.

5 References

1. (a) F. Aquilante, L. De Vico, N. Ferre, G. Ghigo, P. Å. Malmqvist, P. Neogrady, T. B. Pedersen, M. Pitonak, M. Reiher, B. O. Roos, L. Serrano-Andres, M. Urban, V. Veryazov and R. Lindh, *J. Comput. Chem.*, 2010, **31**, 224; (b) L. Ungur and L. F. Chibotaru, SINGLE_ANISO program in MOLCAS (http://molcas.org/documentation/manual/node95.html).
2. B. A. Hess, C. M. Marian, U. Wahlgren and O. Gropen, *Chem. Phys. Lett.*, 1996, **251**, 365.
3. B. O. Roos and P. Å. Malmqvist, *Phys. Chem. Chem. Phys.*, 2004, **6**, 2919.
4. P. Å. Malmqvist, B. O. Roos and B. Schimmelpfennig, *Chem. Phys. Lett.*, 2002, **357**, 230.
5. (a) L. F. Chibotaru, L. Ungur and A. Soncini, *Angew. Chem. Int. Ed.*, 2008, **47**, 4126; (b) L. Ungur, W. V. d. Heuvel and L. F. Chibotaru, *New J. Chem.*, 2009, **33**, 1224; (c) P.-H. Guo, J.-L. Liu, Z.-M. Zhang, L. Ungur, L. F. Chibotaru, J.-D. Leng, F.-S. Guo and M.-L. Tong, *Inorg. Chem.*, 2012, **51**, 1233; (d) G. Novitchi, G. Pilet, L. Ungur, V. V. Moshchalkov, W. Wernsdorfer, L. F. Chibotaru, D. Luneau and A. K. Powell, *Chem. Sci.*, 2012, **3**, 1169; (e) S. K. Langley, L. Ungur, N. F. Chilton, B. Moubaraki, L. F. Chibotaru and K. S. Murray, *Chem. – Eur. J.*, 2011, **17**, 9209.